Force Calculation of Electric Machines with a Flat Air-Gap Using Hybrid Finite Element Mesh

Rong-Jie Wang, Maarten J. Kamper

***Abstract* -- The macro air-gap element and its torque formulation were proposed earlier by Abdel-Razek et al. for modeling electrical machines with an annular air-gap. This paper extends the existing formulation for force calculation in the finite element model incorporating a two-dimensional Cartesian macro air-gap element. The new formulation can be useful for force or torque calculation of some special electric machines with a flat air-gap such as linear and axial flux machines. For validation purpose, the new formulation is implemented to model a single-sided axial flux permanent magnet machine with non-overlap concentrated windings. The solution generated using the new formulation is validated by comparing it with that of the virtual work method and measurements. It shows that the new formulation is computationally efficient and accurate.**

***Index Terms*--Air gaps, finite-element methods, force, linear machines, mesh generation, axial flux machines.**

I. INTRODUCTION

THE finite element dynamic modeling of electrical machines often requires that the relative motion between the stator and the rotor be taken into account. In the past decades, a number of methods and techniques have been developed to handle the movement without re-meshing the computational domain such as the macro air-gap element (AGE), the moving layer method and the Lagrangian multipliers-interpolation method [1].

Amongst others, the macro air-gap element was initially proposed by Abdel-Razek et al. for the dynamic modeling of the annular air-gap of an electrical machine [2, 3]. The prime advantages of the AGE are the ease of handling dynamic motion with great accuracy while the main drawback is the relatively large profile of its stiffness matrix. The later may be alleviated by using a profile optimizing method introduced in [4]. With the availability of greater computing power of personal computers, there has been some renewed interest in AGE [5-10]. The AGE and its torque formulation were originally derived for a polar coordinate system to model an electrical machine with an annular air-gap. To accommodate the two-dimensional modeling of some special electrical machines such as linear and axial flux machines, the Cartesian air-gap element (CAGE) was introduced in [6]. In this paper, the force or torque calculation method presented in [2] has been re-formulated to work with the CAGE. The co-energy method that incorporates the CAGE is also presented in the paper. For validation purposes the new formulation is implemented to model a single-sided axial flux permanent magnet machine with a double-layer non-overlap concentrated winding. The solutions produced by the new formulation are compared with measurements.

This work was supported in part by the National Research Foundation (Incentive funding for rated researcher) and the University of Stellenbosch, all of South Africa.

The authors are with the Department of Electrical and Electronic Engineering, University of Stellenbosch, Private Bag X1, Matieland 7602, South Africa (e-mail: rjwang@ieee.org).

II. FORCE FORMULATION FOR CARTESIAN AIR-GAP ELEMENT

In this section, the force formulations based on the Maxwell stress tensor and the virtual work principle respectively are derived for the two-dimensional CAGE.

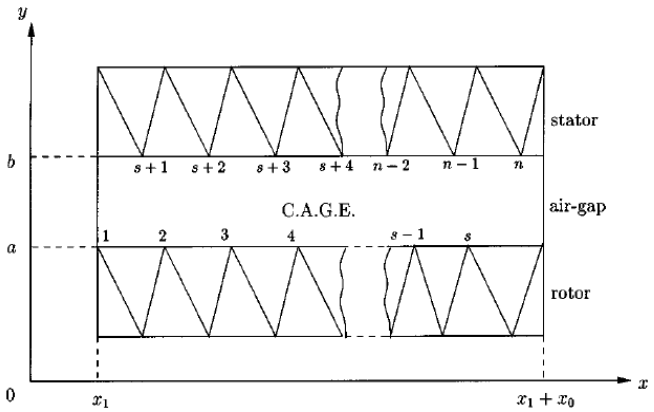

Fig. 1. Solution domain of the CAGE.

A. Maxwell Stress Tensor Method

Consider a generic linear electrical machine, which has a flat air-gap as shown in Fig. 1, where b and a are y-coordinates of the air-gap top and bottom boundaries, respectively. For a Cartesian coordinate system, the electromagnetic force between the stator and rotor of the machine may be expressed as follows by using the Maxwell stress tensor method:

$$F = \frac{p\,L}{2\,\mu_0}\int_{x_1}^{x_1+x_0} B_x B_y dx \tag{1}$$

where p is the number of periodic sections, L is the active length of a coil side of the machine, and x_0 is the periodic length of the CAGE. The flux density components, B_x and B_y, are calculated by using derivatives of the shape function of the CAGE [6], α_i^{ε}, i.e.

$$\alpha_i^{\varepsilon}(x,y) = \frac{y-c}{c'-c}\frac{a_{0i}}{2} + \sum_{n=1}^{\infty}\frac{e^{\lambda_n(y-c)} - e^{\lambda_n(c-y)}}{e^{\lambda_n(c'-c)} - e^{\lambda_n(c-c')}}\left(a_{ni}\cos\lambda_n x + b_{ni}\sin\lambda_n x\right)$$

and

$$c = \begin{cases} a \text{ and } c' = b \text{ if } i \in \{1,2,\ldots,s\} \\ b \text{ and } c' = a \text{ if } i \in \{s+1,\ldots,t\}, \end{cases} \tag{2}$$

where $\lambda_n = \pm 2n\pi / x_0$, a_{0i}, a_{ni} and b_{ni} are Fourier coefficients of the nodal shape function of the CAGE defined from the shape functions of the adjacent triangular elements. Equation (1) is, hence, transformed into the following format:

$$F = \frac{p\,L}{\mu_0}[\mathrm{A}]_{\varepsilon}^{T}[\mathrm{f}][\mathrm{A}]_{\varepsilon}, \tag{3}$$

where $[\mathrm{A}]_{\varepsilon}$ is the nodal vector potential values of the CAGE and [f] is a matrix defined as:

978-1-4244-4175-4/10/$25.00 ©2010 IEEE

$$f_{ij}=\int_{x_1}^{x_1+x_0}\frac{\partial\alpha_i}{\partial x}\frac{\partial\alpha_j}{\partial y}dx=\frac{x_0}{2}\sum_{n=1}^{\infty}\lambda_n{}^2\frac{e^{\lambda_n(y-c)}-e^{\lambda_n(c-y)}}{e^{\lambda_n(c'-c)}-e^{\lambda_n(c-c')}}\frac{e^{\lambda_n(y-g)}+e^{\lambda_n(g-y)}}{e^{\lambda_n(g'-g)}-e^{\lambda_n(g-g')}}(a_{ni}b_{nj}-a_{nj}b_{ni}) \quad (4)$$

where $$g=\begin{cases} b \text{ and } g'=a \text{ if } i\in\{1,2,\ldots,s\} \\ a \text{ and } g'=b \text{ if } i\in\{s+1,\ldots,t\}. \end{cases}$$

Since in (1) force is calculated by means of integration along a closed contour in the air-gap, if we integrate along the mid-line of the air-gap, i.e. $y = (a+b)/2$, (4) becomes:

$$f_{ij}=\frac{x_0}{2}\sum_{n=1}^{\infty}\lambda_n{}^2\frac{\sinh\lambda_n(\frac{a+b}{2}-c)}{\sinh\lambda_n(c'-c)}\frac{\cosh\lambda_n(\frac{a+b}{2}-g)}{\sinh\lambda_n(g'-g)}(a_{ni}b_{nj}-a_{nj}b_{ni}) \quad (5)$$

B. *Virtual Work Method*

The virtual work method makes use of the following formulation:

$$F_{vw}=p\,L\frac{\partial W'}{\partial x}\approx p\,L\frac{\Delta W'}{\Delta x}, \quad (6)$$

where the magnetic co-energy W' consists of two parts as

$$W'=W'_{FE}+W'_{CAGE}=\sum_{i=1}^{total}\int(B\,H-\int H\,dB)dS_i+\frac{1}{2\mu_0}[\mathrm{A}]_\varepsilon^T[\mathrm{S}]_\varepsilon[\mathrm{A}]_\varepsilon \quad (7)$$

The first term is the summation of the magnetic co-energy of each classical triangle element while the second term is the magnetic co-energy of the CAGE, where $[S]_\varepsilon$ is the stiffness terms matrix of the CAGE as given in [6]:

$$S_{ij}^{\varepsilon}=\frac{x_0}{4}\frac{b-a}{(c'-c)(g'-g)}a_{0i}a_{0j}+\frac{x_0}{2}\sum_{n=1}^{\infty}\frac{\lambda_n}{e^{\lambda_n(c'-c)}-e^{\lambda_n(c-c')}}\cdot\frac{1}{e^{\lambda_n(g'-g)}-e^{\lambda_n(g-g')}}\cdot\left[\left(e^{\lambda_n(b-c)}-e^{\lambda_n(c-b)}\right)\left(e^{\lambda_n(b-g)}+e^{\lambda_n(g-b)}\right)-\left(e^{\lambda_n(a-c)}-e^{\lambda_n(c-a)}\right)\left(e^{\lambda_n(a-g)}+e^{\lambda_n(g-a)}\right)\right](a_{ni}a_{nj}+b_{ni}b_{nj}) \quad (8)$$

For a triangle element with nonlinear magnetic properties, the co-energy is obtained through an integration process using the respective B-H curves.

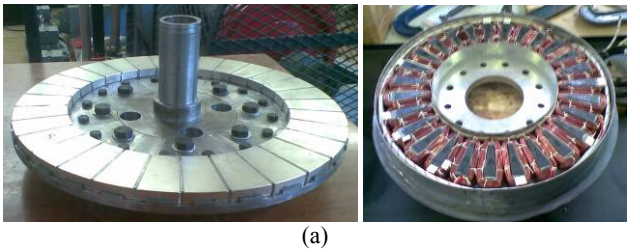

(a)

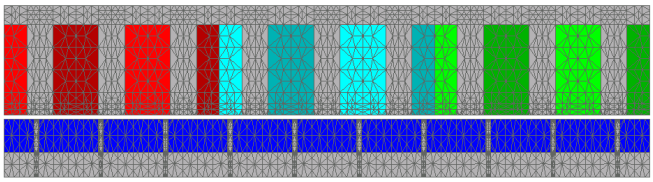

(b)

Fig. 2. Single-sided axial flux permanent magnet machine with double-layer, non-overlap, concentrated winding, (a) physical machine; (b) finite element model.

III. Validation by Comparison

To validate the above-derived force formulation for the CAGE, an axial flux permanent magnet (AFPM) motor with a non-overlap concentrated winding shown in Fig. 2(a) is modeled. The design data and parameters of the AFPM motor are given in Table I.

TABLE I
Design Specifications of The Single-Sided Axial Flux Permanent Magnet Motor

Design data	
Output power, kW	16
Rated speed, r/min	450
Number of phases	3 (Wye)
Rated line current (RMS), A	44
Rated frequency, Hz	112.5
Rated torque, Nm	340
Rated current density (RMS), A/mm^2	11.5
Rated power factor	0.922 (Lagging)
Number of poles	30
Number of stator slots	27
Number of stator coils	27
Number of turns per coil	101
Number of parallel circuits	3
Stator outer diameter, mm	330
Stator inner diameter, mm	224
Total axial length, mm	53.25
Air gap length, mm	1.4
Permanent magnet type	N40SH sintered NdFeB
Magnet arc to pole pitch ratio	0.94
Cooling system	Liquid
Class of insulation	F

The motor is of a double-layer 30-pole/27-slot combination. Fig. 2(b) shows the developed two-dimensional finite element (FE) model of the motor at the average air-gap radius, which consists of 10 poles and 9 coils requiring positive periodicity being applied to the left and right boundaries. Homogeneous Dirichlet conditions are assigned to the top and bottom boundaries. The entire air-gap is represented by a CAGE and is therefore not meshed.

Both the Maxwell stress tensor and the virtual work methods are implemented in the finite element coding. The force calculated for different armature currents and current angles are converted into torque by multiplying it with an average radius. The laboratory measurement setup is shown in Fig. 3, in which the AFPM motor is connected to a geared induction machine drive via a torque sensor.

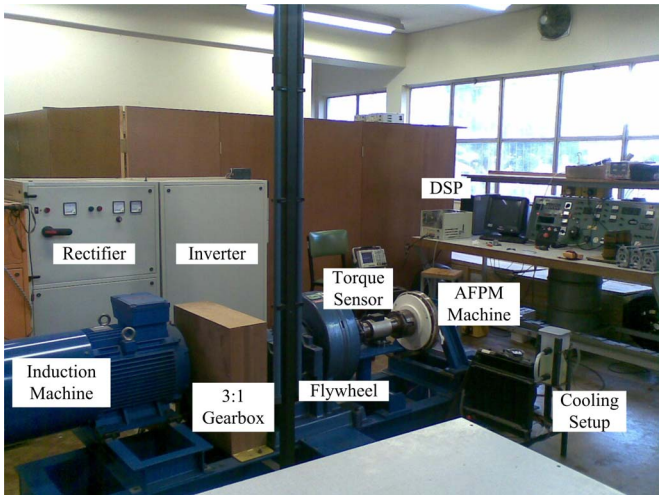

Fig. 3. Laboratory measurement setup.

The geared induction machine drive is controlled to provide loading to the AFPM motor. A DSP controller was used to apply current control of the AFPM motor.

Fig. 4 compares the measured and calculated torque versus current ($i_d=0$) characteristics, while Fig. 5 shows the measured and calculated torque responses to different current angles for 1/3 and 1.0 p.u. current loading.

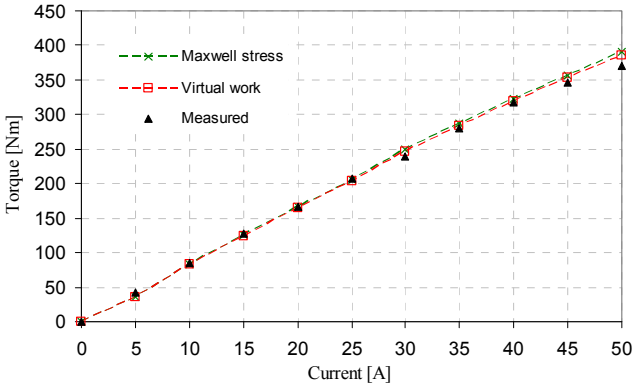

Fig. 4. Torque of the AFPM machine at different armature currents.

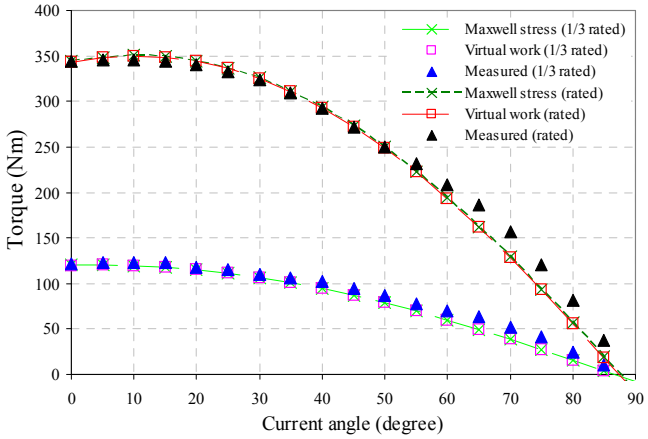

Fig. 5. Torque of the AFPM machine at different current angles with current a parameter.

It can be observed that the calculated results generally correlate well with the measured ones. Both Maxwell stress tensor and virtual work methods give practically the same results; the maximum discrepancy between the two methods is within 0.3%. The FE model consists of 4992 triangle elements and 2874 nodes. The simulation was carried out on a Dell Latitude D830 laptop (Core 2 Duo 2GHz processor) running the SUSE 10.2 operating system. The average CPU time for a single torque calculation (including complete mesh generation, field solution and force calculation sequence) using the Maxwell stress tensor and virtual-work methods are 4 and 5 seconds, respectively.

Although the virtual work method requires two solutions to calculate one torque value (see Eqn. (6)), the solution time is only 20% longer. This is attributed to the fact that a profile reduction scheme devised by [3] is implemented to minimize the re-calculation time of the CAGE stiffness matrix $[S]_\varepsilon$ in (8). Since the CAGE allows for any amount of linear movement, the accuracy of the computed function value [11] and the optimum step size can be easily determined.

IV. Conclusion

In this paper the torque formulation originally derived for the annular air-gap macro element has been re-formulated for Cartesian air-gap element. The new formulation is successfully implemented and validated in a case study. It shows that the torque/force formulation with the CAGE is computationally efficient, accurate and of use to special electrical machines with a flat air-gap.

V. Acknowledgment

The authors acknowledge the contributions of Mr. H.J. Kierstead for his work on the design, construction and measurements of the AFPM prototype machine.

VI. References

[1] F. Rapetti, F. Bouillault, L. Santandrea, A. Buffa and A. Razek, "Calculation of eddy currents with edge elements on non-matching grids in moving structures," *IEEE Trans. Magn*., 36 (2000), pp.1351–1355.

[2] A. A. Abdel-Razek, J. L. Coulomb, M. Feliachi,, and J. C. Sabonnadiere,, "Conception of an air-gap element for the dynamic analysis of the electromagnetic field in electric machines," *IEEE Trans. Magn*., 18 (1982), pp.655–659.

[3] A. A. Abdel-Razek, J. L. Coulomb, M. Feliachi, and J. C. Sabonnadiere, "The calculation of electromagnetic torque in saturated electric machines within combined numerical and analytical solution in the field equations," *IEEE Trans. Magn.*, 17 (1981), pp.3250–3252.

[4] T. J. Flack, and A. F. Volschenk, "Computational aspects of time-stepping finite-element analysis using an air-gap element," in *Proc. Int. Conf. Electr. Mach.*, Paris, France, 1994.

[5] K. Hameyer, R. Mertens, U. Pahner and R. Belmans, "New technique to enhance the accuracy of 2-D/3-D field quantities and forces obtained by standard finite element solutions," *IEE Proc. -Sci. Meas. Technol.,* 145(1998), pp.67-75.

[6] R.-J. Wang, H. Mohellebi, T. J. Flack, M. J. Kamper, J. D. Buys and M. Feliachi, "Two-dimensional Cartesian air-gap element (CAGE) for dynamic finite-element modeling of electrical machines with a flat air gap," *IEEE Trans. Magn.*, 38 (2002), pp.1357–1360.

[7] G. D. Kalokiris, T. D. Kefalas, A. G. Kladas and J. A. Tegopoulos,, "Special air-gap element for 2-D FEM analysis of electrical machines accounting for rotor skew," *IEEE Trans. Magn.*, 41 (2005), pp.2020–2023.

[8] H. De Gersem and T. Weiland, "A computationally efficient air-gap element for 2D FE machine models," *IEEE Trans. Magn.*, 41 (2005), pp.1844–1847.

[9] Z. Belli Boulassel and M. Rachid Mekideche, "Fast dynamic macro element and finite element 2D coupled model for an electromagnetic launcher study," *COMPEL*, 26 (2007), pp.86-97.

[10] D. Zhong and H. Hofmann, "A computationally efficient finite element/analysis model for simulating electric machines with rotor movement," in *Proc. IEEE Energy Conversion Congress and Expo (ECCE)*, San Jose, California, September 20th–24th 2009, pp.3978-3983.

[11] P. E. Gill, W. Murray and M. H. Wright, *Practical optimization,* London: Academic Press, 1981, pp.117-133 and pp.335-338.

VII. Biographies

Rong-Jie Wang received the M.Sc. (Eng.) degree from the University of Cape Town, Cape Town, South Africa, in 1998, and the Ph.D. (Eng.) degree from the University of Stellenbosch, Matieland, South Africa, in 2003. Currently, he is a senior lecturer with the Department of Electrical & Electronic Engineering, University of Stellenbosch. His research interests include special electrical machines, design optimization of electrical machines using finite-element method, thermal modeling of electrical machines, and renewable energy systems. Dr. Wang is a senior member of IEEE and a South African National Research Foundation Supported Researcher.

Maarten J. Kamper received the M.Sc. (Eng.) degree in 1987 and the Ph.D. (Eng.) degree in 1996 from the University of Stellenbosch, Matieland, South Africa. He has been with the academic staff of the Department of Electrical & Electronic Engineering, University of Stellenbosch, since 1989, where he is currently a Professor of electrical machines and drives. His research interests include computer-aided design and control of reluctance, permanent magnets, and induction electrical machine drives. Prof. Kamper is a South African National Research Foundation Supported Researcher and a Registered Professional Engineer in South Africa.